Inverse structure functions

Bruce R. Pearson[1,2] and Willem van de Water[1]
[1]*Physics Department, Eindhoven University of Technology, Postbus 513, 5600 MB Eindhoven, The Netherlands*
[2]*School of Mechanical, Materials and Manufacturing Engineering, University of Nottingham, Nottingham NG7 2RD, United Kingdom*
(Received 20 August 2004; published 15 March 2005)

While the ordinary structure function in turbulence is concerned with the statistical moments of the velocity increment Δu measured over a distance r, the inverse structure function is related to the distance r where the turbulent velocity exits the interval Δu. We study inverse structure functions of wind-tunnel turbulence which covers a range of Reynolds numbers $\mathrm{Re}_\lambda = 400-1100$. We test a recently proposed relation between the scaling exponents of the ordinary structure functions and those of the inverse structure functions [S. Roux and M. H. Jensen, Phys. Rev. E **69**, 16309 (2004)]. The relatively large range of Reynolds numbers in our experiment also enables us to address the scaling with Reynolds number that is expected to highlight the intermediate dissipative range. While we firmly establish the (relative) scaling of inverse structure functions, our experimental results fail both predictions. Therefore, the question of the significance of inverse structure functions remains open.

DOI: 10.1103/PhysRevE.71.036303 PACS number(s): 47.27.Gs, 47.27.Jv, 52.25.Gj, 89.75.Da

I. INTRODUCTION

The discovery that turbulent velocity signals possess a highly nontrivial scaling structure has been an important stimulus to turbulence research. In the well-known Kolmogorov framework, turbulence is viewed as strictly self-similar with a single scaling exponent which is reflected in the $k^{-5/3}$ behavior of the energy spectrum $E(k)$ [2]. It has now become clear that the statistical properties of turbulent fluctuations are much richer. More precisely, statistical moments of the velocity increments $\Delta u(r) = u(x+r) - u(x)$ measured over a distance r exhibit algebraic behavior $\langle [\Delta u(r)]^p \rangle \sim r^{\zeta(p)}$ with scaling exponents $\zeta(p)$ that depend in a nonlinear fashion on the moment p [2], and that are most probably universal, i.e., they do not depend on the detailed realization of the turbulent flow.

Although the scaling properties of the u component of the velocity difference measured in the same (x) direction offer a quite restricted view of turbulence, it is an interesting question whether we can turn the scaling argument around. That is, how long does it take on average for the velocity u to exit a given velocity interval $[u(x) - \Delta u/2, u(x) + \Delta u/2]$ with size Δu? The exit at $x+r$ then defines the *exit distance r*.

The question then is whether moments of the fluctuating exit distances r depend algebraically on the size of the velocity interval

$$\langle r^p \rangle \sim \Delta u^{\theta(p)}, \tag{1}$$

and, if so, what the relation is between the exponents $\theta(p)$ of the inverse structure function and the exponents $\zeta(p)$ of the ordinary structure function.

The inverse structure functions were first proposed by Jensen [1] who found algebraic behavior of the moments $\langle r^p \rangle$ for a turbulent velocity field that was generated by a shell model. No such algebraic behavior was found in [3], where inverse structure functions were computed from an experimental turbulent velocity signal that was obtained at a Reynolds number $\mathrm{Re}_\lambda \approx 2000$. This absence of scaling was explained in [3] by arguing that the moments of the exit distances r probe the episodes in the turbulent flow where viscosity starts to reign (the so-called intermediate dissipative range). As inverse structure functions encompass the crossover of the inertial range to the dissipative range, no algebraic behavior is expected. Instead, as will be explained below, the inverse structure functions are expected to scale with Reynolds number in a special manner. Such scaling was indeed observed in [3]. As [3] had only experimental data at a single Reynolds number, lower-Reynolds-number data were mimicked by filtering the signal at decreasing low-pass frequencies. Because this is not the proper way to alter the Reynolds number, an experimental check of the proposed Reynolds number scaling is still needed.

Recently Jensen and Roux [4] have proposed an exact relation between the ordinary and inverse scaling exponents. The relation, which was proved to hold for binomial measures, reads

$$-\theta(-\zeta(p)) = p. \tag{2}$$

This relation was checked in [4] for a turbulent signal that was obtained by integrating the Gledzer-Ohkitani-Yamada (GOY) shell model [5]; in this case it was shown to hold remarkably well. The problem is that a check of Eq. (2) necessitates the computation of negative moments of either the exit distances r for the inverse structure functions or the velocity increments Δu for the normal structure functions.

To make this explicit, we write Eq. (2) in the form

$$-\zeta(-p) = \theta^{-1}(p). \tag{3}$$

Clearly, the inverse scaling functions $\theta^{-1}(p)$ for positive moments p must now be compared to negative moments of the ordinary structure functions. Jensen and Roux [4] showed that this could actually be done for turbulence generated by the GOY model. The found agreement with Eq. (3) is remarkable because it is well known that for actual turbulence velocity increments, be they from experiments or from direct numerical simulations, negative moments $\langle \Delta u^p \rangle$ with

$p \leqslant -1$ do not exist. This follows from the observation that there is nothing special about the velocity increment 0, and the probability density function of Δu is a constant near $\Delta u = 0$.

The purpose of the present paper is to check Eq. (2), but not through negative moments of the exit distances r. We will demonstrate that, contrary to the velocity increments, the probability density function of the exit distances vanishes at $r=0$, so that negative moments make sense. A second purpose of this paper is a check of the Reynolds number scaling of inverse structure functions that was proposed in [3]. The key idea is that inverse structure functions probe the dissipative large wave number end of the energy cascade. Unlike the ordinary structure functions, which can be scaled with the Kolmogorov length and velocity, the scaling of the inverse structure functions should now involve the Reynolds number explicitly.

II. EXPERIMENTS

We have analyzed both normal and inverse structure functions of wind-tunnel turbulence where in a single experimental facility a rather large range of Reynolds numbers ($\mathrm{Re}_\lambda = 400-1100$) was covered. The streamwise velocity component was acquired in a turbulent wake from a multiscale grid, which has been described in [6]. This grid is located in the NTNU [7] recirculating wind tunnel, which has a test section of $2.7 \times 1.8\ \mathrm{m}^2$ cross section and length 11 m. The signals are measured 40 mesh lengths downstream of the grid using the constant-temperature anemometry hot-wire technique. At this location $\langle u^2 \rangle^{1/2}/U = 0.16$ and is R_λ independent. At each Reynolds number, long (6×10^4 integral times) time series of two velocity components at a single point were registered. In order to control the noise, which is a crucial point in inverse structure functions, the signals were always filtered at the Kolmogorov frequency f_K, $f_K = U/(2\pi\eta)$, where η is the Kolmogorov length scale and U is the mean velocity, and sampled at f_s, with $f_s > 2 f_K$. Throughout, we translate times t into separations x using Taylor's frozen turbulence hypothesis, $x = Ut$, where U is the mean velocity.

Characterizing a signal through the statistics of exit lengths is similar to (but not the same as) characterizing a signal through its zero crossings. In this case it is known [8] that noise contamination has a large effect. We expect, therefore, that noise is also important for exit lengths, for example, the signal may accidentally exit from a given interval through noise fluctuations which then cut a long exit length into shorter pieces.

From the registered signals of a one-dimensional signal of a single velocity component, inverse structure functions were computed using two algorithms. In the first algorithm (I) we fix the size Δu of the velocity interval and start from the velocity u_1 at position x_1, which determines the interval $[u_1 - \Delta u/2, u_1 + \Delta u/2]$. We then register the position x_2 when the velocity signal first exits this interval. This defines the exit length $r_1 = x_2 - x_1$. At position x_2 we repeat the procedure, and so on. The statistics of the collected exit lengths r_i, $i = 1, \ldots,$ are improved by restarting at several initial positions x_1. Next, the procedure is repeated at another value of Δu.

In algorithm II we start the quest for exit lengths at all considered values of Δu at the same position x and stop once the velocity signal exits at the given Δu. Also here the statistics is improved by randomly picking starting positions x. The difference between both algorithms is that in case I the exit position x_2 defines the start of the new interval $[u_2 - \Delta u/2, u_2 + \Delta u/2]$, contrary to case II where all intervals at a given Δu start at random positions.

In both cases we collect histograms of exit lengths r_i, $i = 1, 2, \ldots$, at each Δu. From these histograms we form the probability density functions $P_{\Delta u}(r)$ from which the moments are computed,

$$\langle r^p \rangle = \int_0^\infty r^p P_{\Delta u}(r)dr \Bigg/ \int_0^\infty P_{\Delta u}(r)dr. \tag{4}$$

Although it may be contended that algorithm I is biased toward the short exit lengths, both algorithms give, up to a prefactor of $\langle r^p \rangle$, the same results; that is, the scaling properties of r^p computed using either method I or II are the same. There is a slight influence of the chosen method on the scaling of the negative moments, but it does not affect our conclusions.

III. INVERSE STRUCTURE FUNCTIONS

Typical inverse structure functions for $p=1,2$ are shown in Fig. 1(b). In order to facilitate the comparison to the more familiar ordinary structure functions which are shown in Fig. 1(a), we plot the dependent variable $\langle r^p \rangle^{1/p}$ on the horizontal axis and the independent variable Δu on the vertical axis. While the ordinary structure functions of Fig. 1(a) exhibit unambiguous algebraic behavior, no such scaling can be observed for the inverse structure functions and it is not possible to assign a scaling exponent $\theta(p)$ [9].

The absence of scaling agrees with [3], but disagrees with the inverse structure functions that were computed from a one-dimensional turbulent field generated by a shell model [1]. A first remarkable result is that the inverse structure functions show *relative* scaling. This is demonstrated in Fig. 2 where we plot $\langle r^p \rangle^{1/p}$ as a function of $\langle r \rangle$ for $p=2,3,\ldots,8$. From these plots it is possible to determine *relative* scaling exponents $\tilde{\theta}(p)$ as

$$\langle r^p \rangle^{1/p} = \langle r \rangle^{\tilde{\theta}(p)/p}.$$

In the case that also $\langle r^p \rangle \sim (\Delta u)^{\theta(p)}$, these relative scaling exponents will be related to the true ones as $\tilde{\theta}(p) = \theta(p)/\theta(1)$

By setting $\tilde{\theta}(p=1)$ to the value $\theta(p=1)$ which was found in [1], we may compare our exponents with those of [1]. There is a striking agreement between the (relative) experimental exponents and the ones obtained from the model signal. From Fig. 2(b) it appears that both $\tilde{\theta}(p)$ and $\theta(p)$ are linear functions of the order p. Therefore, inverse structure functions are not sensitive to intermittency. Intermittency breaks the self-similarity of the moments, which is reflected in a *nonlinear* dependence of the ordinary structure function exponents $\zeta(p)$ on the order p.

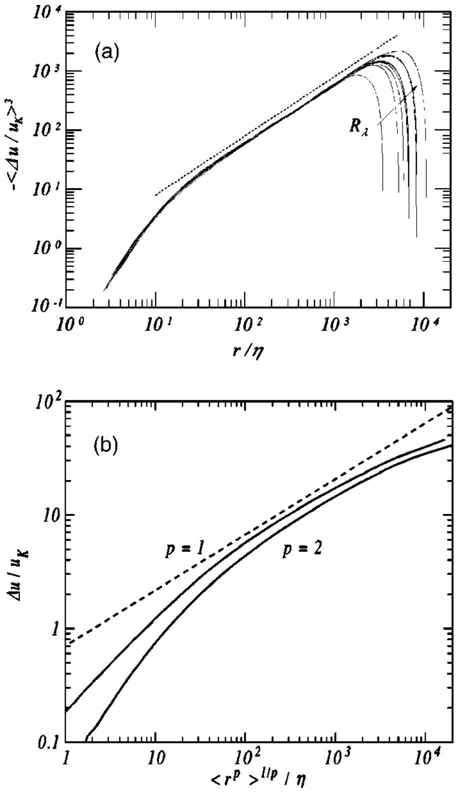

FIG. 1. (a) Full lines: ordinary third-order structure functions for a range of Reynolds numbers $\mathrm{Re}_\lambda = 400-1100$ demonstrating the scaling behavior of the data. Dashed line: the exact relation $\langle (\Delta u / u_K)^3 \rangle = -4/5(r/\eta)$, where u_K is the Kolmogorov velocity. (b) Full lines: inverse structure functions for the highest Reynolds number $\mathrm{Re}_\lambda = 1120$. In order to facilitate the comparison with (a), the dependent variable $\langle r^p \rangle^{1/p}/\eta$ for $p=1$ and 2 has been plotted on the horizontal axis, and the independent variable $\Delta u / u_K$ on the vertical axis. Dashed line: scaling behavior found in [1], $\langle r \rangle \simeq \Delta u^{2.04}$

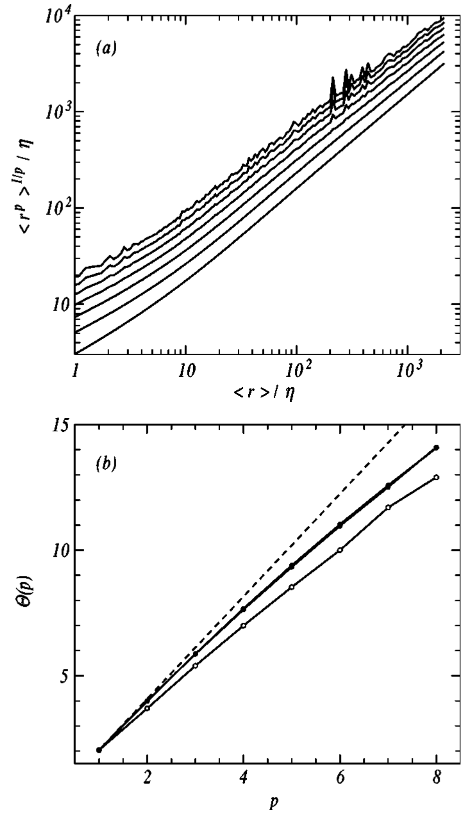

FIG. 2. (a) Inverse structure functions with moments $p = 2, 3, \ldots, 8$ plotted as a function of moment $p=1$ for a Reynolds number $\mathrm{Re}_\lambda = 1120$. (b) Open circles, scaling exponents $\theta(p)$ from inverse structure functions of shell model data [1]; closed dots, *relative* exponents $\widetilde{\theta}(p)$ of inverse structure functions from experiments at $\mathrm{Re}_\lambda = 1121$ and 508. They have been normalized to $\theta(1) = 2.04$. Dashed line: $\widetilde{\theta}(p) = 2.04\, p$.

The verification of the inversion formula Eq. (2) is a problem as it involves negative moments. For small velocity increments, the probability density function (PDF) of Δu is nearly Gaussian: nothing special happens at $\Delta u = 0$. Therefore, negative moments with $p \leqslant -1$ do not exist for the ordinary structure functions in our experiment. However, vanishing velocity increments have vanishing exit distances r, and negative moments may be computed from the probability density functions of exit distances. This property of the PDF's of exit distances was already demonstrated by Jensen [1] for turbulence generated by the GOY shell model, and it is again demonstrated for our experiment in Fig. 3 for Δu ranging from dissipative to inertial range values.

It can be concluded from Fig. 3 that for increments Δu larger than the Kolmogorov velocity, negative moments with $p \gtrsim -2$ exist. This contrasts with the case of the velocity increments at a fixed separation which correspond to the ordinary structure function. As Fig. 3 also illustrates, the PDF of Δu is flat near $\Delta u = 0$, and, consequently, negative moments with $p \leqslant -1$ do not exist [10]. Therefore, we will check the inversion formula Eq. (2) in the form

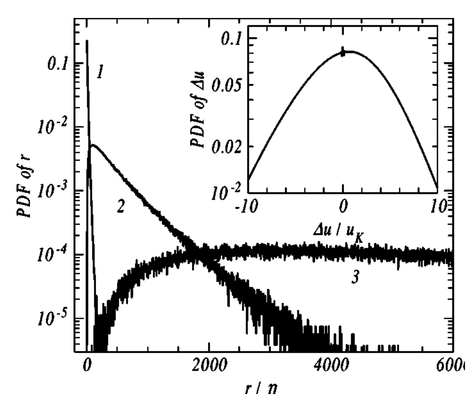

FIG. 3. Probability density functions of exit distances r/η for velocity increments $\Delta u / u_K = 0.85$, 11 and 50, for curves 1, 2, and 3, respectively. Inverse structure functions are moments of these PDF's. Inset: probability density function of velocity increments Δu at a fixed separation $r/\eta = 110$. This PDF corresponds to the normal structure function. While the PDF's of exit distances support negative moments, no negative orders with $p < -1$ exist of the ordinary structure function.

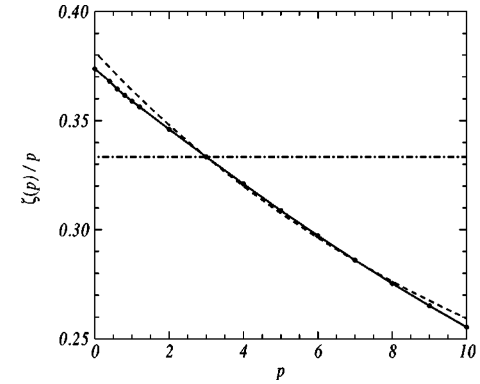

FIG. 4. Dots: scaling exponents $\zeta(p)/p$ measured in a turbulent flow with $\mathrm{Re}_\lambda = 8\times 10^2$. The actually measured $\zeta(3)=1.06$, but the exponents were normalized such that $\zeta(3)=1$. Dashed line: log-Poisson model [12]. Dash-dotted line: Kolmogorov self-similar prediction $\zeta(p)=p/3$.

$$\frac{\theta(-p)}{p} = -\frac{\zeta^{-1}(p)}{p}, \quad p > 0, \tag{5}$$

where $\zeta^{-1}(p)$ is the inverse of the exponent function $\zeta(p)$ of the ordinary structure function. Because the functions $\theta(p)$ and $\zeta(p)$ both trivially become 0 at $p=0$, and we compute negative orders $\theta(p)$ for small p, we have divided both left- and right-hand sides of Eq. (3) by p. We will argue below that for small p, $\zeta(p)/p$ and, similarly, the ratio $\zeta^{-1}(p)/p$ contain relevant information about turbulent velocity fluctuations. If the inversion formula Eq. (5) holds, the exact result for $\zeta(3)$ fixes $\theta(-1)=3$.

For a turbulent flow at $\mathrm{Re}_\lambda = 800$ that was stirred using a similar grid as in the experiments reported in this paper, Fig. 4 shows the scaling exponents $\zeta(p)/p$. As was already emphasized in [11], it is clear that intermittency not only shows in the high-order moments, but also in the low-order ones. Since the sign of Δu has no special meaning in inverse structure functions, at least not in the current definition, we computed the ordinary structure functions using absolute value increments $|\Delta u|$, which enables us to measure structure functions of noninteger order $p<1$, even those at $p=0$ (which is $\lim_{p\to 0}\langle |\Delta u|^p\rangle^{1/p} = \exp\langle \ln|\Delta u|\rangle$). Figure 4 also shows that the log-Poisson model of [12] gives an excellent parametrization of the experiments. Instead of the actually measured data, we will therefore use this model to determine the inverse function $\zeta^{-1}(p)$.

From measured PDF's of exit distances we computed a few low-order negative moments. As for the positive ones, also the inverse structure functions at negative orders lack scaling behavior, and we plot in Fig. 5(a) the inverse structure functions in a relative way. Also the negative order inverse structure functions display self-similar behavior and $\theta(-p)/p$, shown in Fig. 5(b), is almost constant and equal to the (set) reference value at $p=1$, $\theta(-1)=3$. On the contrary, the inverse moments of the ordinary structure function $-\zeta^{-1}(p)/p$ strongly depend on the order p, which reflects the intermittency of the turbulent velocity signal. The trend of the two curves is actually opposite and demonstrates that the

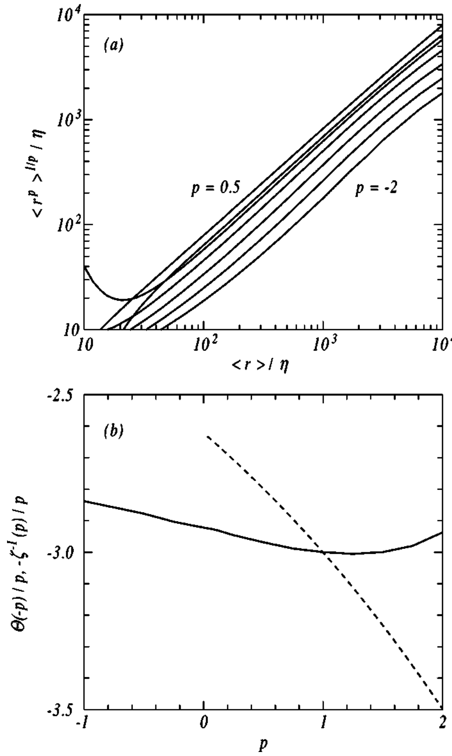

FIG. 5. (a) Inverse structure functions for orders $p=-2,-1.5,-1,-0.5,-0.1,0.1,0.5$ for a turbulent velocity signal at $\mathrm{Re}_\lambda=1100$. (b) Dashed line, $-\zeta^{-1}(p)/p$ computed from the log-Poisson model [12]; full line, relative exponents $\widetilde{\theta}(-p)/p$ from the inverse structure functions in (a). If the inversion formula Eq. (3) were to work for turbulence experiments, the dashed and full curves would have collapsed.

inversion formula Eq. (2) that links the inverse to the ordinary structure function cannot hold for experimental turbulence.

Surprisingly, the inversion formula in the form of Eq. (3) was successfully checked for very large (up to order −12) negative orders of the ordinary structure function by Jensen and Roux [4]. It is clear from the arguments presented here that this cannot be done for experimental turbulence. Moreover, in the form where all moments exist, the inversion fails. Therefore, the significance of the inverse structure functions and its relation to the ordinary structure function of experimental turbulence signals remain unsettled.

IV. INTERMEDIATE DISSIPATIVE RANGE

Let us now turn to the overall shape of the inverse structure functions. Ordinary structure functions display algebraic behavior with scaling exponents $\zeta(p)$ that depend on p in a nonlinear fashion. The power and beauty of the multifractal model [2] is its explanation of this behavior in terms of a distribution $f(\alpha)$ of local singularities α such that locally velocity increments scale as $\Delta u(r) \sim (r/L)^\alpha$, where we have also introduced the integral scale L. The distribution of singularities defines the structure function $G_p(r) = \langle [\Delta u(r)]^p\rangle$ through the integral

$$\frac{\langle[\Delta u(r)]^p\rangle}{u_K^p} \sim \int_{\alpha_{\min}}^{\alpha_{\max}} (r/L)^{3-f(\alpha)+p\alpha} d\alpha, \tag{6}$$

which is done over the local scaling exponents α. For $r/L \ll 1$, that is, inertial range scales, the integrand is sharply peaked at the value α^* where the exponent $3-f(\alpha)+p\alpha$ is minimal. If α^* is contained in the interval $[\alpha_{\min},\alpha_{\max}]$, the integral is determined by the value of the exponent in the point $\alpha=\alpha^*$, and does not depend on its bounds. As a consequence, the structure function is algebraic with scaling exponent set by $\zeta(p)=3-f(\alpha^*)+p\alpha^*$, with corrections logarithmic in r/L.

The integration over α runs from the strongest $(\alpha_{\min})$ to the weakest $(\alpha_{\max})$ singularity strength of the turbulent velocity field. In fact, the weakest singularity that can be seen is set by the viscosity and r/L. It is reached when the eddy turnover time equals the viscous dissipation time,

$$\alpha_{\max} = \frac{1 + 4\ln(r/\eta)/\ln \mathrm{Re}}{3 - 4\ln(r/\eta)/\ln \mathrm{Re}}. \tag{7}$$

For small enough r, $\alpha_{\max}$ may become smaller than α^* and the integral Eq. (6) is determined explicitly by $\alpha_{\max}$. Since $\alpha_{\max}$ depends logarithmically on r, the structure function is no longer algebraic and thus lacks scaling behavior. As the argument r now always appears in the combination $\ln(r/\eta)/\ln\mathrm{Re}$, the structure functions at different Reynolds numbers must no longer be plotted as [2]

$$\ln(G_p/u_K^p) \quad \text{versus} \quad \ln(r/\eta), \tag{8}$$

but as

$$\frac{\ln(G_p/u_K^p)}{\ln \mathrm{Re}} \quad \text{versus} \quad \frac{\ln(r/\eta)}{\ln \mathrm{Re}}. \tag{9}$$

The scaling Eq. (9) of structure functions thus is characteristic for the intermediate dissipative range of separations r. Such scaling has been observed in spectra of temperature fluctuations in strongly turbulent thermal convection [13]. Since the inverse structure functions are thought to probe the smooth episodes of the velocity field, it has been proposed [3] that they should scale with Reynolds number in the way described by Eq. (9).

The problem with an experimental check of Eq. (9) is that it depends on the *logarithm* of the Reynolds number and a large range of Reynolds numbers is needed to distinguish it from the more mundane scaling Eq. (8). Our Reynolds numbers range from $\mathrm{Re}_\lambda=400$ to 1100, but $\ln 1100/\ln 400$ is a mere 1.17. Therefore, the normalization Eq. (9) stretches both horizontal and vertical axes only by a factor 1.17, for the inverse structure function at $\mathrm{Re}_\lambda=1100$, compared to the one at $\mathrm{Re}_\lambda=400$; this is a small effect. However, it is important to realize that all our data were acquired in the same experimental facility, with all the signals filtered exactly at the Kolmogorov frequency; for these data the only varying parameter is the Reynolds number.

The question now is whether we can distinguish in the experiment the ordinary scaling Eq. (8) from the scaling with the logarithm of the Reynolds number Eq. (9). For inverse structure functions of order $p=1$ these distinct scalings are shown in Figs. 6(a) and 6(b), respectively. In both cases the curves collapse, but the collapse is better for the ordinary scaling Eq. (8).

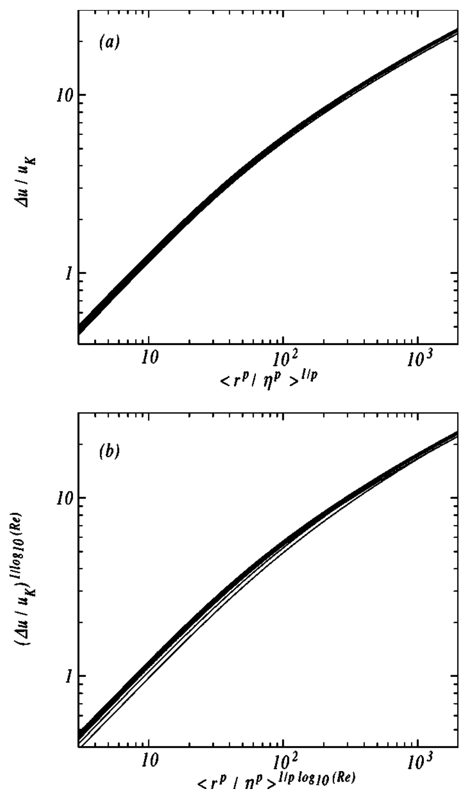

FIG. 6. Inverse structure functions of order $p=1$ and Reynolds numbers $\mathrm{Re}_\lambda=425, 508, 673, 829, 862, 969, 1008, 1038, 1096, 1121$, respectively. (a) Plotted in the standard way, Eq. (8). (b) Using the intemediate dissipative range scaling scaling Eq. (9) [which is $(r/\eta)^{1/\mathrm{Re}_\lambda}$, $(\Delta u/u_K)^{1/\mathrm{Re}_\lambda}$ on a logarithmic axis). The scaling was done relative to the curve at $\mathrm{Re}_\lambda=1121$.

We conclude that the experiment favors the ordinary scaling of the inverse structure function, indicating that the inverse structure function is not especially sensitive to the intermediate dissipative range. However, we realize that the difference between the two scalings Eqs. (8) and (9) is small. Our conclusion is at variance with that of [3], but they have analyzed the effect of varying low-pass filtering on only a single experimental time series, which cannot substitute for genuine variation of the Reynolds number.

In testing Eq. (9) it must be realized that purely algebraic inverse structure functions that pass through the fixed point $(r/\eta, \Delta u/u_K)=(1,1)$ are up to a stretch factor invariant under the scaling of Eq. (9). Therefore, the interval in r/η where the scaling Eq. (9) holds can be selected by an appropriate change of units. The inverse structure functions of Fig. 6 can be roughly approximated by algebraic behaviors at both small and large r. It appears that the large r algebraic behavior approximately passes through this fixed point. As the inverse structure functions already collapse at large r in Fig. 6(a), they will remain doing so in Fig. 6(b). This allows us to focus on the small r behavior (the intermediate dissipative range) where the collapse of the curves is poorest with the scaling Eq. (9).

V. CONCLUSION

The fractal character of strong turbulence is reflected in intermittency: the tendency of turbulence to fill space unevenly with local singularities. Intermittency is missed by inverse structure functions which have (relative) scaling exponents that depend linearly on the order. It is therefore not surprising that we fail to verify the inversion formula Eq. (2) relating these exponents to the ones from the ordinary structure functions which *do* reflect intermittency and, instead, depend nonlinearly on the order.

The scaling exponents of (relative) inverse structure functions appear to be well defined and agree with the ones obtained from a turbulent velocity time series that was generated by a shell model [1]. The wide open question is what these exponents mean. Clearly, inverse structure functions capture something from a turbulence signal that cannot be obtained from the ordinary structure functions, but we do not know what it is.

We find a clear distinction between the statistics of velocity signals in the experiment and the velocities in the GOY shell model [1,4]. For the latter, inverse structure functions scale with scaling exponents that can be inverted. Perhaps this is because the experiment is a one-dimensional cut through one component of the velocity field, while for the shell model the computed field is all there is.

By performing experiments at a relatively large range of Reynolds numbers, we have also refuted a recent suggestion that inverse structure functions are sensitive to the intermediate dissipative range [3]. Although the inverse structure function captures little of truly structural aspects of turbulence, it is an interesting quantity and further work is clearly needed to understand it.

The statistics of signals of a single velocity component in a point of the turbulent field keeps posing intriguing questions. However, we must also realize that this is only a small part of the full story. The turbulent velocity field has three components and evolves in space and time. Some of this rich structural information was already ignored in this paper when we defined moments in terms of the absolute value of the velocity increments, $\langle|\Delta u(r)|^p\rangle$, which ignores the essential connection for $p=3$ between the skewness of the velocity increments and the cascade of energy toward small scales. Only recently was an attempt made to include structural information in the definition of scaling exponents [14].

ACKNOWLEDGMENTS

We thank P.-Å. Krogstad and the Department of Applied Mechanics, Thermo & Fluid Dynamics of the Norwegian University of Science & Technology in Trondheim for making available the wind-tunnel facility. We also thank Mogens Jensen for discussions which inspired this article. We gratefully acknowledge financial support by the "Nederlandse Organisatie voor Wetenschappelijk Onderzoek (NWO)" and "stichting Fundamenteel Onderzoek der Materie (FOM)."

[1] M. H. Jensen, Phys. Rev. Lett. **83**, 76 (1999).
[2] U. Frisch, *Turbulence: The Legacy of A. N. Kolmogorov* (Cambridge University Press, Cambridge, U.K., 1995).
[3] L. Biferale, M. Cencini, D. Vergni, and A. Vulpiani, Phys. Rev. E **60**, R6295 (1999).
[4] S. Roux and M. H. Jensen, Phys. Rev. E **69**, 016309 (2004).
[5] E. B. Gledzer, Sov. Phys. Dokl. **18**, 216 (1973); M. Yamada and K. Ohkitani, J. Phys. Soc. Jpn. **56**, 4210 (1987); Prog. Theor. Phys. **79**, 1265 (1988).
[6] B. R. Pearson, P.-A. Krogstad, and W. van de Water, Phys. Fluids **14**, 1288 (2002).
[7] Norwegian University of Science & Technology in Trondheim.
[8] K. R. Sreenivasan, A. Prabhu, and K. Narashimha, J. Fluid Mech. **137**, 251 (1983).
[9] In a recent paper, S. Beaulac and L. Mydlarski [Phys. Fluids **16**, 2126 (2004)], report measurements of low-order inverse structure functions in wind-tunnel turbulence. Although their structure functions look similar to ours, it was concluded that the inverse structure functions show scaling in the interval $10^2 \lesssim r/\eta \lesssim 10^3$, and a direct scaling exponent was assigned which agreed well with those found in [1] for turbulence generated by a shell model.
[10] Very near $\Delta u=0$ a small feature is seen in the experimental PDF in Fig. 3, but this is due to a well documented effect of the differential nonlinearity of an analog to digital converter, together with the nonlinear velocity to voltage calibration; see J. A. Herweijer, F. C. van Nijmweegen, K. Kopinga, J. H. Voskamp, and W. van de Water, Rev. Sci. Instrum. **65**, 1786 (1994).
[11] K. R. Sreenivasan, S. I. Vainshtein, B. Bhiladvala, I. San Gil, S. Chen, and N. Cao, Phys. Rev. Lett. **77**, 1488 (1996).
[12] Z-S. She and E. Leveque, Phys. Rev. Lett. **72**, 336 (1994).
[13] X-Z. Wu, L. Kadanoff, A. Libchaber, and M. Sano, Phys. Rev. Lett. **64**, 2140 (1990).
[14] V. S. L'Vov, E. Podivilov, and I. Procaccia, Phys. Rev. Lett. **79**, 2050 (1997); I. Arad, B. Dhruva, S. Kurien, V. S. L'Vov, I. Procaccia, and K. R. Sreenivasan, *ibid.* **81**, 5330 (1998); I. Arad, V. S. L'Vov, and I. Procaccia, Phys. Rev. E **59**, 6753 (1999); A. Staicu, B. Vorselaars, and W. van de Water, *ibid.* **68**, 046303 (2003).